Advanced Materials '93, I / B: Magnetic, Fullerene, Dielectric, Ferroelectric,
Diamond and Related Materials, edited by M. Homma et al.
Trans. Mat. Res. Soc. Jpn., Volume 14B

© 1994 Elsevier Science B.V. All rights reserved.

Growth and characterization of epitaxial $SrTiO_3$ thin films with supereminent polarizability

M. Iwabuchi, K. Matsui, M. Taga and T. Kobayashi

Faculty of Engineering Science, Osaka University,
1-1 Machikaneyama-cho, Toyonaka, Osaka 560, Japan

Epitaxial $SrTiO_3$ (STO) thin films were grown on (111)Pt/(100)MgO substrate successfully by the rf magnetron sputtering. The dielectric constant of 110-nm-thick STO thin films reached as high as $370\epsilon_0$ at room temperature. Cr/(100)STO/(111)Pt MIM' structures were prepared with various STO thicknesses ranging 39~262 nm for the investigation of STO electrical features. Leakage current vs. voltage curves of the MIM' structure showed the rectifying property. Herein two possible band diagram of aforementioned MIM' structure can be proposed. However by considering the capacitance vs. voltage curves of them, the band diagram where STO layer include no space-charge was concluded as a much proper one.

1. INTRODUCTION

STO is an incipient ferroelectric. It has high dielectric constant of more than $300\epsilon_0$ even at room temperature, and the value increases steeply to a few tens of thousands at cryogenic temperatures. [1] Moreover, it does not show hysteresis property. Owing to these incipient ferroelectricities, STO attracts the attention to use not only for a thin-film capacitor in Si large-scale integration but also for a gate insulator of the metal-insulator-superconductor (or semiconductor) field effect transistors (MISFETs) with extremely high carrier concentration. [2]

In regard to the STO thin films, to obtain higher value of the dielectric constant is a current goal. Besides, to confirm the band diagrams of STO layer is thought to be essential for the advance of many applications. Thus far, the voltage dependence of leakage current (I-V curves) of metal-STO-other metal MIM' structure has been obtained by many groups. [3, 4] , which showed the rectifying property. From this result, Abe *et al.* proposed a band model of the Cr/STO/Pt MIM' structure where Schottky barrier was comprised in the STO layer. [4] However, this model is thought to fail in compatibility with the capacitance vs. voltage curves (C-V curves) of it.

In this paper we report the extremely high dielectric constant of epitaxial (100)STO thin films grown by the rf magnetron sputtering. Then close examinations are given to those films from electrical point of view. Eventually, we conclude the band diagram free from the space-charges has a strong validity.

2. EXPERIMENTAL

(111)Pt was grown epitaxially by the electron beam evaporation on a (100)MgO substrate at 570 °C first. Then, STO thin films were deposited on the Pt/MgO substrate by the rf magnetron sputtering, in an atmosphere of 5 Pa O_2 and 5 Pa Ar. The substrate temperature was 540 °C and the input rf power was 0.38 W/cm^2. Finally, Cr electrodes (0.0257 mm^2) were deposited on the STO films by the resistive-heated evaporation. The I-V and the C-V characteristics of the specimens were observed at room temperature. Measuring frequency of the capacitance was 1 MHz. After all electrical measurements, the STO films were etched off by HF acid selectively, and then covered by gold for the purpose of subsequent measurement of STO thicknesses of our specimens by using scanning tunneling microscope (STM). Grown STO thicknesses were observed to be ranged from 35 to 2620 Å.

3. RESULTS AND DISCUSSION

Figure 1 is the C-V characteristics of the specimens with various STO thicknesses, w. This figure indicates the internal electric field dependence of the STO dielectric constant which is maximum

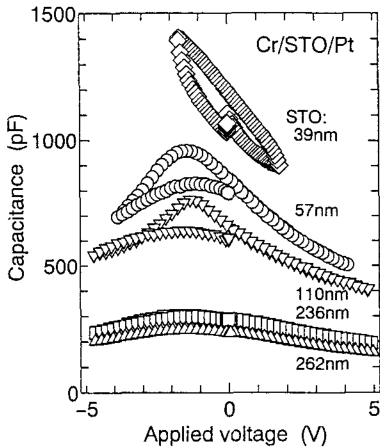

Figure 1. Capacitance vs. voltage curves with various $SrTiO_3$ thicknesses.

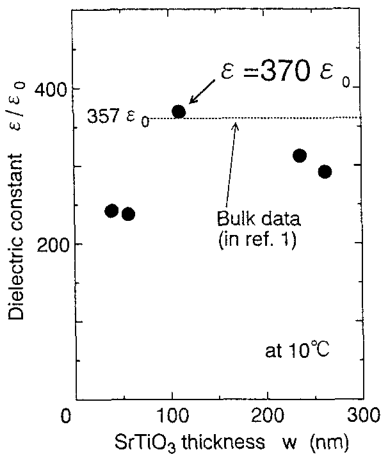

Figure 2. Dielectric constants of various $SrTiO_3$ thicknesses.

with zero internal field. Therefore the capacitance shows the largest value when $-1 \sim -2$ V is applied to the upper Cr electrode which corresponds to the work function difference between Cr and Pt.

By using the elementary equation of a parallel-plate capacitor,

$$C_{max} = \epsilon_{STO} S/w, \tag{1}$$

the dielectric constant of the STO layer, ϵ_{STO}, can be deduced, where S is the area of the Cr electrode.

Figure 2 indicates the deduced dielectric constants of the STO films. We obtained $370\epsilon_0$ with the 110-nm-thin film, which is the highest value reported so far. Actually, the dielectric constant of (100)-oriented STO single-crystal bulk is $\sim 357\epsilon_0$ at 10 °C, being comparable or a bit lower than our present result. [1] Consequently, we think to be reaching the top limit of the dielectric constant of STO thin films.

Generally, the thinner the STO thickness, the more difficult it is to get the high dielectric constant. [5] It might be due to an incorporation of thin degraded layer with low dielectricity at the interface between Pt and STO, which was introduced during the deposition process. Recently, the Fourier transform infrared (FTIR) spectra which reflect the crystallinity were observed about the ultra thin STO films by 35 Å. Some changes of the absorption peak in the spectra due to the degraded layer were expected to appear in the FTIR measurement. Actually, as we make the STO thinner less than 110 Å, the absorption peak broadened to the higher wavenumbers. It intimates the existence of the degraded layer on the interface. The degraded layer is thought to play a role of a series parallel-plate capacitor and pull down the total value of the capacitance. Despite of this general difficulty, our STO layer shows extremely high dielectric constant of $240\epsilon_0$ with 39-nm-STO thickness.

To date, rectifying I-V curves have been obtained of some M-STO-M' [4] or metal-STO-superconductor MIS junctions. [2, 3] We also observed the same result as for the Cr/STO/Pt structure. From these rectifying curves, a group suggested a band model of the MIM' structure where the STO film served as an n^+-type semiconductor and Schottky barrier existed inside the STO layer [4] as is shown in Fig. 3. In actual fact, this model can explain the rectifying property undoubtedly.

However, it is worth noting that another ordinary band model which includes no space-charge, on the other hand, is not inconsistent with the asymmetric I-V curves yet. This model drawn in Fig. 4(a) can agree well with the rectifying action as following way. As to ordinary oxide insulators, such as SiO_2, the leakage current property determined mainly by the tunneling effect. However,

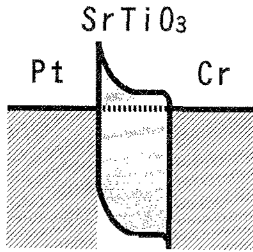

Figure 3. Possible band diagram of Cr/STO/Pt structure. STO layer contains space-charges.

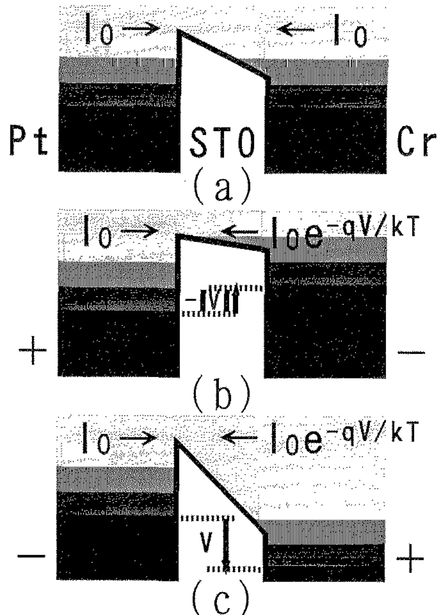

Figure 4. Possible band diagram and the rectification of Cr/STO/Pt structure. STO layer has no space-charge. (a)No bias voltage, (b)negative and (c)positive bias voltages are applied to Cr.

comparing the energy gap of STO single crystal with that of SiO_2, STO has much smaller value of ~3.2 eV, although SiO_2 has as large as 8.8 eV energy gap. In addition, the electron affinity of the STO single crystal is close to that of Cr. [6] Then the leakage current property is thought to be ruled by another mechanism. Figure 4 represents the rectifying action of the Cr/STO/Pt structure. In the equilibrium state at zero bias as illustrated in Fig. 4(a), the net current is zero. When the negative or positive voltages applied to Cr as shown in Figs. 4(b) and 4(c), the carrier distribution is changed according to Boltzmann statistics generally. If the current direction from Cr to Pt is chosen as positive, the leakage current, I, is given by,

$$I = -I_0\{\exp(-qV/(k_BT) - 1\}, \quad (2)$$

where I_0 is the saturation current, q the elementary charge, k_B the Boltzmann constant and T the temperature. This expression ignores the injection property of carriers to the STO layer from the side metals, and the scattering effect inside the STO layer for simplicity. This leakage current characteristic of this space-charge-free model is identical with that of the aforementioned Schottky barrier model. Finally, as long as in regard to the I-V curve, there is no difference between two models.

We focus on the C-V property next. There is, on the other hand, a pronounced difference. Figure 5(a) shows the theoretical C-V curves of the Schottky band model. In the calculation, we treated the STO layer as an n^+-type semiconductor to form the Schottky barrier inside the STO layer. the Schottky barrier height, $q\phi_b$, was put to be about 1 eV in favor of the other group's experimental result. As to the dielectric constant, we used our experimental data which depended strongly on the electric field as shown in Fig. 1. About other parameters for STO, we chose pertinent values as follows: temperature T: 300 K, measuring frequency: 1 MHz, density of donors N_d: 1×10^{19} /cm^3, and mobility μ: 7 cm^2/(V·s).

In Fig. 5(a), there are three curves of different thicknesses of the STO layer. The density of donors looks large, but if we set this number smaller, the depletion width, d, increases proportionally to the reciprocal of the square root of the donor concentration. And if the number is small enough, the depletion layer reaches the thickness of STO film, w, and exceeds it. In the present condition, the density of donors is large enough for thinner depletion layer than 50-nm-STO film at zero bias voltage. However, despite of this large number of donors, d can reach w by applying reverse (it is positive in the Fig. 5(a)) bias voltages. This behavior is drawn in the same figure for 50-nm-thick STO layer. After the depletion layer touches the Cr electrode metal, the aspect of this C-V curve changes. Inversely, if we make

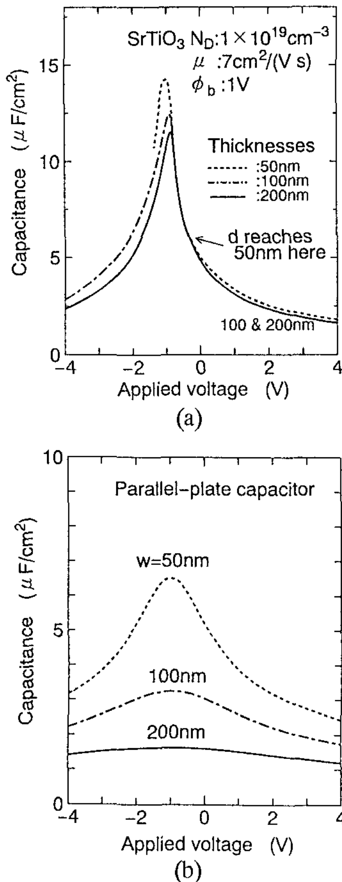

Figure 5. Theoretical capacitance vs. voltage curves. (a)Schottky band model and (b)space-charge free model.

the number of the density larger to fit to the experimental results, it may be impossible to measure the capacitance because of the large current leakage.

In Fig. 5(a), one can see slight decrease of the maximum capacitance as the thickness becomes larger. it is inconsistent completely with the experimental result (see Fig. 1). In actual fact, the experimental result exhibits that C_{max} is in the inverse-proportion-rule against the STO thickness. Moreover one can see steep grades of these theoretical curves. It stems from not only the internal field dependence of the STO dielectric constant, but also the rapid change of the depletion layer width against the applied voltage. This feature is not consistent with the experimental one, neither.

On the contrary, we also consider the fitness of the later band model free from space-charges. Figure 5(b) shows its theoretical *C-V* curves. In these calculations, the Cr/STO/Pt structure is equivalent to a parallel-plate capacitor. In this figure, one can see the inverse-proportion-rule of the capacitance against the STO thickness which can be easily described by the Eq. (1). The characteristics of these curves resemble our experimental result (see Fig. 1) and others' pretty well. Finally, we conclude that the STO thin films is without space-charges substantially, and we strongly support this space-charge-free band diagram of Fig. 4(a) as a much proper one.

4. CONCLUSIONS

Epitaxial (100)STO thin films were grown successfully by the rf magnetron sputtering on (111)Pt/(100)MgO substrate. The dielectric constant of the STO films reached as high as $370\epsilon_0$ at room temperature. The *I-V* and *C-V* curves of the Cr/(100)STO/Pt MIM' structure were obtained with various STO thicknesses ranging 39~262 nm. By comparing them with theoretical results, two possible band models with and without space-charges were discussed, and finally, we conclude the band diagram which has no space-charge is much proper one for the description of Cr/(100)STO/Pt MIM' structure.

REFERENCES

1. R. C. Neville, B. Hoeneisen and C. A. Mead, J. Appl. Phys. **43**(1972) 2124
2. T. Fujii, K. Sakuta, T. Awaji, K. Matsui, T. Hirano, Y. Ogawa and T. Kobayashi, Jpn. J. Appl. Phys. **31**(1992) L612
3. A. Walkenhorst, C. Doughty, X. X. Xi, S. N. Mao, Q. Li and T. Venkatesan, Appl. Phys. Lett. **60**(1992) 1744
4. K. Abe and S. Komatsu, Jpn. J. Appl. Phys. **31**(1992) 2985
5. T. Kuroiwa, T. Honda, H. Watarai and K. Sato, Jpn. J. Appl. Phys. **31**(1992) 3025
6. V. E. Henrich, G. Dresselhaus and H. J. Zeiger, Phys. Rev. B **17**(1978) 4908